Distribution of singular values in large sample cross-covariance matrices

Arabind Swain

Department of Physics, Emory University, Atlanta, GA 30322, USA

Sean Alexander Ridout

Department of Physics, Emory University, Atlanta, GA 30322, USA and
Initiative in Theory and Modeling of Living Systems, Atlanta, GA 30322, USA

Ilya Nemenman

Department of Physics, Emory University, Atlanta, GA 30322, USA
Department of Biology, Emory University, Atlanta, GA 30322, USA and
Initiative in Theory and Modeling of Living Systems, Atlanta, GA 30322, USA

(Dated: February 19, 2025)

For two large matrices $\mathbf{X}$ and $\mathbf{Y}$ with Gaussian i.i.d. entries and dimensions $T \times N_X$ and $T \times N_Y$, respectively, we derive the probability distribution of the singular values of $\mathbf{X}^T\mathbf{Y}$ in different parameter regimes. This extends the Marchenko–Pastur result for the distribution of eigenvalues of empirical sample covariance matrices to singular values of empirical cross-covariances. Our results will help to establish statistical significance of cross-correlations in many data-science applications.

I. INTRODUCTION

Many data-science applications require detecting correlations between two variables X and Y of dimensions N_X and N_Y, respectively, with $N_X, N_Y \gg 1$. When these variables are sampled T times, with $T \sim N_X, N_Y$, sampling fluctuations can produce spurious correlations, even when X and Y are truly uncorrelated. Characterizing these sampling-induced correlations is essential before isolating genuine signals in real datasets.

Marchenko and Pastur famously analyzed similar correlations in sample self-covariance matrices [1], deriving their eigenvalue distribution using now-classic methods of Random Matrix Theory (RMT) [2]. For $T > N_X, N_Y$, later work generalized these results to cross-correlations of whitened variables [3–5]. However, to our knowledge, no comparable results exist for the unwhitened cross-covariance between X and Y and arbitrary relations between T, N_X, and N_Y, though some related results have been calculated [6–8].

In this paper, we derive the eigenvalue spectra of unwhitened cross-covariance matrices for uncorrelated Gaussian i.i.d. data and arbitrary relations among T, N_X, and N_Y. We hope that these can then be used to distinguish signal from sampling noise in data science applications.

II. MODEL AND METHODS

We consider T samples of random variables X and Y combined into matrices $\mathbf{X}$ and $\mathbf{Y}$, with dimensions $T \times N_X$ and $T \times N_Y$, respectively. The entries of $\mathbf{X}$ and $\mathbf{Y}$ are i.i.d. Gaussian random variables with zero mean and variances σ_X^2 and σ_Y^2 respectively,

$$X_{t\mu} \sim \mathcal{N}(0, \sigma_X^2), \quad Y_{t\nu} \sim \mathcal{N}(0, \sigma_Y^2), \tag{1}$$

$$t = 1, \ldots, T, \ \mu = 1, \ldots, N_X, \ \nu = 1, \ldots, N_Y, \tag{2}$$

so that the measured correlations in X and Y vanish asymptotically, as $N_X/T, N_Y/T \to 0$.

We define normalized matrices as

$$\widetilde{\mathbf{X}} = \frac{\mathbf{X}}{\sigma_X}, \qquad \widetilde{\mathbf{Y}} = \frac{\mathbf{Y}}{\sigma_Y}. \tag{3}$$

For $T \gg 1$, each column in these matrices has variance of nearly one. Note that, in typical applications, $\sigma_{X/Y}$ would be estimated from samples as well, and the estimates might be different from their true value. Here we disregard this distinction, as in [6], arguing that sampling fluctuations in estimating scalar parameters are negligible compared to sampling effects on the thermodynamically many singular values.

The normalized empirical cross-covariance matrix (NECCM) $\mathbf{C}$ is then

$$\mathbf{C} = \frac{1}{T} \widetilde{\mathbf{Y}}^T \widetilde{\mathbf{X}}, \tag{4}$$

which has dimensions $N_Y \times N_X$. If $N_X \neq N_Y$, this matrix is not square, but it obviously has the same nonzero singular values as its transpose. Without loss of generality, in all calculations, we take $N_X \leq N_Y$.

We want to calculate distribution of these singular values. To utilize RMT methods, most of which only work for square symmetric matrices, we focus instead on eigenvalues of

$$\mathbf{C}^T\mathbf{C} = \frac{1}{T^2} \widetilde{\mathbf{X}}^T \widetilde{\mathbf{Y}} \widetilde{\mathbf{Y}}^T \widetilde{\mathbf{X}}. \tag{5}$$

Nonzero eigenvalues of $\mathbf{C}^T\mathbf{C}$, which we denote as λ, are the same as nonzero eigenvalues of $\mathbf{C}\mathbf{C}^T$, and their distribution is related to the distribution of nonzero singular values of $\mathbf{C}$, denoted as γ, via

$$\rho_C(\gamma) = 2\sqrt{\lambda}\rho_{C^TC}(\lambda), \quad \gamma = \sqrt{\lambda}. \tag{6}$$

The distribution further contains a delta function at zero, corresponding to the zero eigenvalues of $\mathbf{C}^T\mathbf{C}$ when $N_X \leq N_Y$.

To explore the problem in different regimes, we define:

$$q_X \equiv N_X/T, \; q_Y \equiv N_Y/T, \; p_X \equiv 1/q_X, \; p_Y \equiv 1/q_Y. \quad (7)$$

Eigenvalue density. We compute the eigenvalue density of the square of the NECCM, Eq. (5), by computing its Stieltjes transform, as is the standard approach [2]. The Stieltjes transform of a matrix A is defined as

$$g_{A,N}(z) = N^{-1}\mathrm{Tr}(z\mathbf{I} - \mathbf{A})^{-1}, \quad (8)$$

where z is a complex number. We denote the large-N limit of $g_{A,N}$ by $\mathfrak{g}_\mathbf{A}$ [2]. The eigenvalue density is obtained from the Sokhotski–Plemelj formula

$$\rho_A(\lambda) = \frac{1}{\pi}\lim_{\eta \to 0^+} \Im\mathfrak{g}_\mathbf{A}(z = \lambda - i\eta), \quad (9)$$

where $\Im$ denotes the imaginary part. We use a series of relatively common random matrix operations to obtain the Stieltjes transform of the square of NECCM, in the limit where $N_X, N_Y, T \to \infty$ with p_X and p_Y held fixed. These steps are outlined in the *Appendix*.

As the imaginary part of the Stieltjes transform gives us the eigenvalue density of the square of the NECCM, evaluating the discriminant involved in solving an algebraic equation for the Stieltjes transform (see *Appendix*) gives the boundaries of the range, in which the eigenvalue density is nonzero. These boundaries are denoted by $\lambda_\pm$. The corresponding values for nonzero singular values of NECCM are denoted by $\gamma_\pm$. Analytical expression for these boundaries for the cross-covariance spectrum of pure uncorrelated noise are one of the central results of this paper.

Numerical simulations. We confirm our results by simulating the model, Eq. (1), numerically. Although the eigenvalue density is expected to be self-averaging, and thus our calculations for $\rho(\gamma)$ will be exact for SVD of an *individual* matrix for sufficiently large T, making T very large substantially increases the computational costs. Thus, we simulate matrices with $T = 1000$, and more precisely test our predictions by averaging over 500 independent realizations.

III. EQUATION FOR STIELTJES TRANSFORM AND SINGULAR VALUE DENSITY BOUNDS

We calculate the density of eigenvalues of the square of NECCM in 3 cases, covering all possible relationships between T, N_X, N_Y: (1) $T > N_X, \; N_Y$, (2) $N_Y \geq T \geq N_X$, and (3) $T < N_X, \; N_Y$. For analyzing these different cases, we note that the square of the NECCM can be written as an $N_X \times N_X$ matrix $\frac{1}{T^2}\widetilde{\mathbf{X}}^T\widetilde{\mathbf{Y}}\widetilde{\mathbf{Y}}^T\widetilde{\mathbf{X}}$ or an $N_Y \times N_Y$ matrix $\frac{1}{T^2}\widetilde{\mathbf{Y}}^T\widetilde{\mathbf{X}}\widetilde{\mathbf{X}}^T\widetilde{\mathbf{Y}}$. Both of these matrices will have the same nonzero eigenvalues. Similarly, the $T \times T$

matrix $\mathbf{H} = \frac{1}{T^2}\widetilde{\mathbf{X}}\widetilde{\mathbf{X}}^T\widetilde{\mathbf{Y}}\widetilde{\mathbf{Y}}^T$ will have the same nonzero eigenvalues.

While nonzero eigenvalues of all of these matrices are the same, the total number of eigenvalues is different. For example, the Stiltjes transform $\mathfrak{h}$ of $\mathbf{H}$ gives the density for T eigenvalues of the $T \times T$ matrix, of which only $\min(T, N_X)$ are nonzero. The total number of eigenvalues in $\mathbf{C}^T\mathbf{C}$ and $\mathbf{CC}^T$ is N_X and N_Y, respectively. Thus, the eigenvalue densities of the three matrices are not the same. To relate densities to each other, we need to subtract the δ functions at zero, and then rescale the densities of nonzero eigenvalues to one in all three cases.

With this, we write the finite size Stieltjes transform of $\mathbf{C}^T\mathbf{C}$:

$$g_{\mathbf{C}^T\mathbf{C}, N_X}(z) = \frac{1}{N_X}\left(T\frac{1}{T}\sum_{\mu=1}^{T}\frac{1}{z - \lambda_\mu} + \frac{N_X - T}{z}\right)$$

$$= \frac{1}{N_X}\left(T\,h_T(z) + \frac{N_X - T}{z}\right) \quad (10)$$

$$= p_X h_T(z) + (1 - p_X)\,\delta(z), \quad (11)$$

where λ_μ are the T eigenvalues of $\mathbf{C}^T\mathbf{C}$ and $h_T(z) \equiv g_{\mathbf{H},T}(z)$. A similar expression, with N_X and N_Y swapped, holds for $\mathbf{CC}^T$.

An RMT calculation (Appendix A) then shows that the Stieltjes transform $\mathfrak{h}$ of $\mathbf{H}$ satisfies a cubic equation

$$a\mathfrak{h}^3 + b\mathfrak{h}^2 + c\mathfrak{h} + d = 0, \quad (12)$$

where

$$a = z^2 p_X p_Y, \quad (13)$$
$$b = z\left(p_Y(1 - p_X) + p_X(1 - p_Y)\right), \quad (14)$$
$$c = ((1 - p_X)(1 - p_Y) - z p_X p_Y), \quad (15)$$
$$d = p_X p_Y. \quad (16)$$

Thus, solving Eq. (12), and then using Eq. (11), gives the eigenvalue density of $\mathbf{C}^T\mathbf{C}$, which can be used to compute the density of the nonzero singular values of the cross-covariance using Eq. (6).

A. Spectrum of empirical cross covariance matrix when $T < N_X, \; N_Y$

The cubic polynomial given by Eq. (12) can be solved, numerically or analytically, for the imaginary part of $\mathfrak{h}$ at any parameter values. Taking its imaginary part then gives us the density of nonzero eigenvalues.

Here, we solve the equation numerically (which we refer to as the "semi-analytic" solution, since it solves numerically the analytical expression, Eq. (12)), and study the spectrum for a variety of parameter regimes. The spectrum has compact support, showing a single band of eigenvalues with upper and lower edges. The edges can be calculated by finding the condition under which the the discriminant of the cubic equation, Eq. (12), becomes
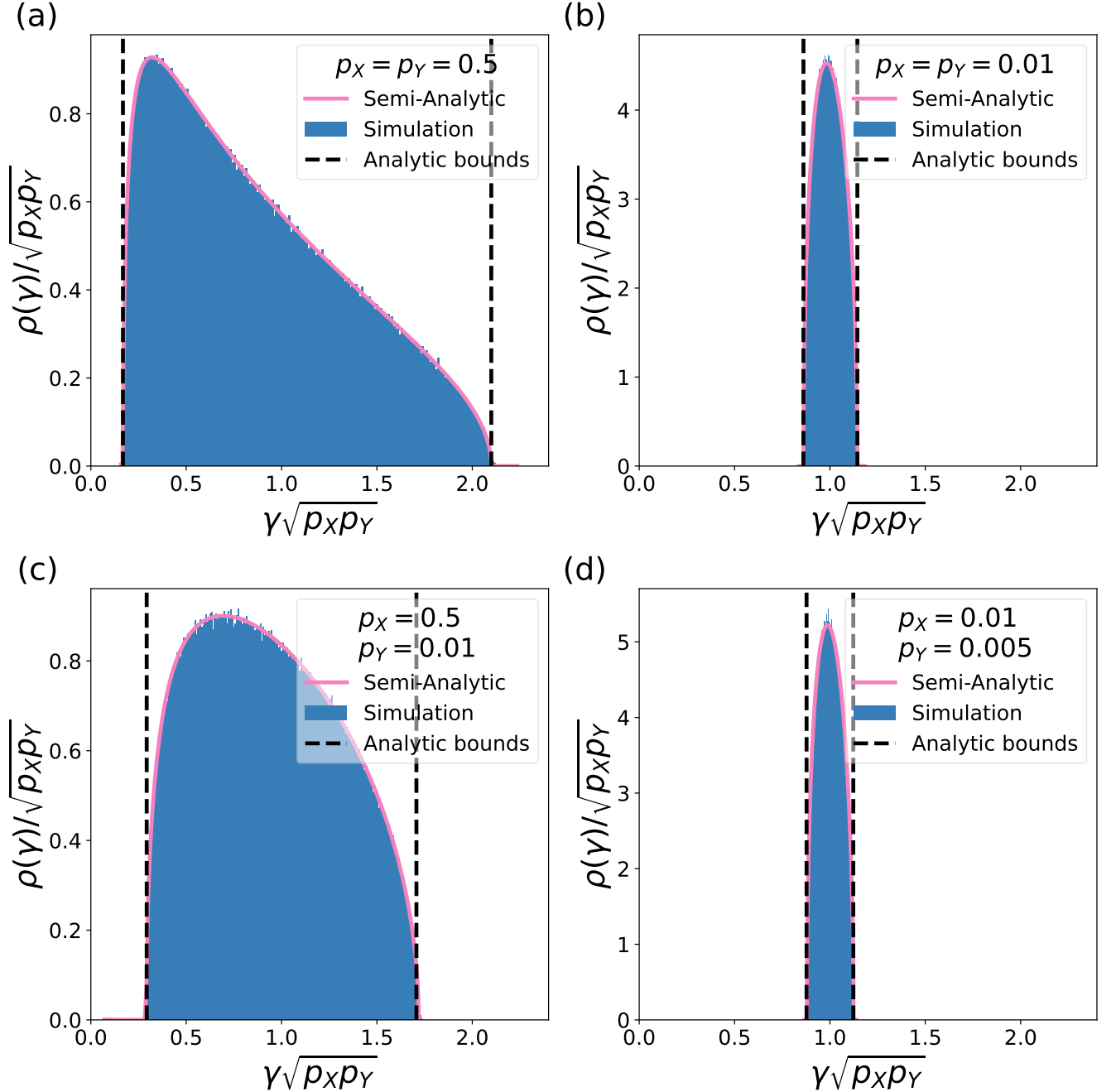
Figure 1. Distribution of nonzero eigenvalues for $T < N_X$, N_Y. **(a)** $p_X = p_Y = 0.5$, **(b)** $p_X = p_Y = 0.01$, **(c)** $p_X = 0.5$, $p_Y = 0.01$, and **(d)** $p_X = 0.01$, $p_Y = 0.05$. The blue bars are the histogram of the simulated data. The magenta curve is computed from the numerical solution of the exact cubic equation for the Stiltjes transform. The black dotted lines show edges of the nonzero part of the density in simplifying limits, evaluated analytically. Here, $T = 1000$, and the the numerical simulation for spectrum consists of 500 independent model realizations.

zero. To get easily interpretable formulas for the edges $\lambda_\pm$ (and hence $\gamma_\pm$), we take various simplifying limits where the discriminant equation for the cubic polynomial is exactly solvable.

For the case where $p_X = p_Y$ (same-size data matrices), the bounds for the nonzero singular value density then

become

$$\gamma_\pm = \sqrt{\frac{8p_X^2 + 20p_X^3 - p_X^4 \pm p_X^{5/2}(8+p_X)^{3/2}}{8p_X^4}}. \quad (17)$$

Assuming $p_X = p_Y \to 0$ (so that we are in the severely undersampled regime, where the number of samples is

much smaller than the number of dimensions in X and Y), the edge values become

$$\gamma_\pm \approx \frac{1}{p_X}(1 \pm \sqrt{2p_X}).\qquad(18)$$

For the case where $p_Y = \epsilon p_X$, where $\epsilon \to 0$, but $p_X = O(1) < 1$ the bounds are

$$\gamma_\pm \approx \sqrt{\frac{1 + p_X \pm 2\sqrt{p_X}}{\epsilon p_X^2}}.\qquad(19)$$

Finally, for $p_Y = \alpha p_X$, where $p_X \to 0$ and $\alpha < 1$ (both X and Y are extremely undersampled, but unequal in size), the bounds are

$$\gamma_\pm \approx \frac{1 \pm \sqrt{p_Y + p_X}}{\sqrt{p_Y p_X}}.\qquad(20)$$

We see that, in all of these limits, the center of the singular value distribution is approximately the geometric mean of the inverse aspect ratios, $\sqrt{\frac{1}{p_X p_Y}} = \sqrt{q_X q_Y}$. This sets the typical scale of sampling noise singular values at a given sample size T. The noise eigenvalues of $\tilde{\mathbf{X}}^T\tilde{\mathbf{X}}/T$ and $\tilde{\mathbf{Y}}^T\tilde{\mathbf{Y}}/T$ individually scale like q_x and q_y [1]. Thus, this scaling is plausible if each eigendirection is poorly-sampled enough that they can be found to correlate with each other by chance: evidently, since $N/T = O(1)$, this is the case.

Figure 1 compares our analytical results to numerical simulations for the density of singular values γ of $\mathbf{C}$. We scale the singular values by the scale factor $\sqrt{\frac{1}{p_X p_Y}}$. We see that the semi-analytic solution for the density is in excellent agreement with our numerical results. Further, we see that the analytical solutions for the bounds, in appropriate limits, also agree well with simulations.

The simulations and the semi-analytic solutions also agree for other parameter values where simple analytic bounds for the edges could not be evaluated exactly (see Appendix A).

B. Spectrum of empirical cross covariance matrix when $N_Y \geq T \geq N_X$

Solving for the roots of the cubic polynomial in Eq. (12) and taking its imaginary part again gives us the density of nonzero eigenvalues.

In this case, we can evaluate the edges of the spectrum exactly in the limit $p_Y = \epsilon p_X$, where $\epsilon \to 0$, and $p_X = O(1) > 1$. In this case, the bounds are

$$\gamma_\pm = \sqrt{\frac{1 + p_X \pm 2\sqrt{p_X}}{\epsilon p_X^2}}.\qquad(21)$$

This limit is the same as in the case when $T \leq N_X$, N_Y, although the densities differ by a constant factor between these cases.
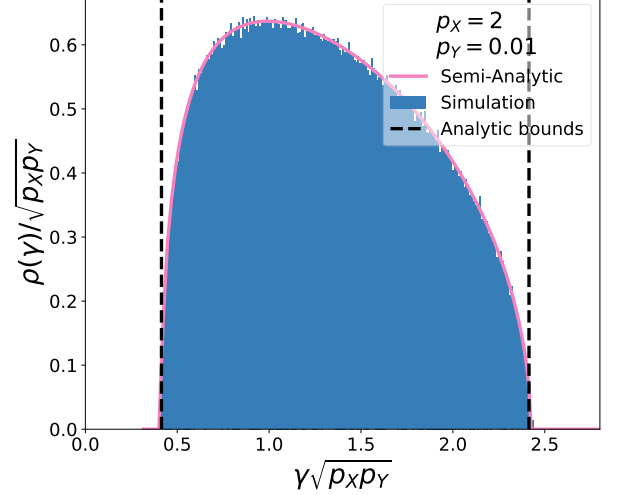

Figure 2. Distribution of nonzero eigenvalues for $N_Y \geq T \geq N_X$, specifically, $p_X = 2$, $p_Y = 0.01$. Plotting conventions are the same as in Fig. 1. Here, again, $T = 1000$, and the numerical simulation for spectrum consists of 500 independent model realizations.

Figure 2 shows that the semi-analytic solution for the density, and the analytic solution for the edges, match our numerical simulations in this case as well.

C. Spectrum of empirical cross covariance matrix for $T > N_X, N_Y$

Solving for the roots of the cubic polynomial, Eq. (12), and taking its imaginary part again gives us the density of nonzero eigenvalues. We then obtain simplified formulas for $\gamma_\pm$ in limiting cases.

For the case where $p_X = p_Y$, the discriminant of the cubic equation for $\mathfrak{h}$ is a 5th-order polynomial with three zero solutions and two nonzero solutions, given by $z_\pm = \frac{8p_X^2 + 20p_X^3 - p_X^4 \pm p_X^{5/2}(8 + p_X)^{3/2}}{8p_X^4}$. Now because $z_- < 0$ and the squares of singular values are always positive, the upper bound of the non-zero density is z_+ but the lower bound is 0. Thus the bounds for the nonzero eigenvalue density are

$$\gamma_+ = \sqrt{\frac{8p_X^2 + 20p_X^3 - p_X^4 + p_X^{5/2}(8 + p_X)^{3/2}}{8p_X^4}}, \quad \gamma_- = 0.\qquad(22)$$

In the limit $p_X \gg 1$ (extremely good sampling), this simplifies to $\gamma_+ \approx \sqrt{\frac{3}{2p_X}} = \sqrt{\frac{3q_X}{2}}$. Thus, in this limit the scaling of the edges agrees with those for the cross-correlations of whitened variables evaluated in Ref. [3], where $\gamma_+ = 2\sqrt{q_X}$, and $\gamma_- = 0$. Note, however, that the exact value of the upper edge is different for the whitened cross-correlation matrices, because the self-covariances
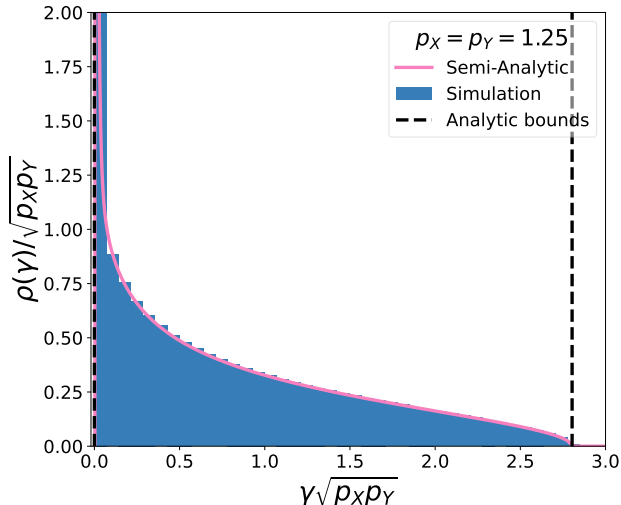
Figure 3. Distribution of nonzero eigenvalues for $T > N_X, N_Y$, specifically $p_X = p_Y = 1.25$. Plotting conventions are the same as in Fig. 1. Here, again, $T = 1000$, and numerical simulation for spectrum consists of 500 independent model realizations.

used for whitening also fluctuate.

Figure 3 shows that these limiting formulas for the edges, and the semi-analytic solution for the spectrum match numerical simulations.

IV. DISCUSSION

We have used random matrix theory to calculate the density of singular values of normalized cross-correlation matrices. Further, in simplifying limits, we were able to obtain simple, exact formulas for the edges of the spectrum.

In all cases, the scale of the non-zero singular values is given roughly by $1/\sqrt{p_X p_Y} = \sqrt{N_X N_Y}/T$. Thus, the noise, unsurprisingly, decreases as more samples are collected, relative to the dimensions of the two observed variables. More surprisingly, however, this calculation in fact suggests that the cross-covariance can sometimes be used to detect a signal which is not detectable from either the covariance of X or that of Y alone, as recently observed numerically [9].

To see this, consider a naïve protocol for establish a correlation between high-dimensional X and Y: we first search for a low-dimensional signal in X (e.g., using principle component analysis), then search for a low-dimensional signal in Y, and finally correlate the low-dimensional signals. The edges of the empirical covariance spectra of X and Y are of order $1/p_X$ and $1/p_Y$, respectively. Thus, a shared signal which has $O(1)$ magnitude in both X and Y will correspond to an outlier eigenvalue outside of the spectrum, and hence can be de-

tected if $T > N_X, N_Y$. In particular, if $N_Y > T > N_X$ (one variable is well sampled, and one variable is poorly sampled), the signal in X cannot be detected. Since the noise spectrum of $\mathbf{C}$ depends on the geometric mean $\sqrt{p_X p_Y}$, however, the same signal may be detectable in $\mathbf{C}$, if X is sampled well enough to "make up for" the poor sampling of Y. Making this rough analysis precise requires a full calculation of the spectrum of a model with both a signal and noise, which we will present in a future work.

These results also suggest that a sufficiently strong signal can be detected even if $T < N_X, N_Y$.

In the limit $T \gg N_X, N_Y$, where the covariances of X and Y are both well sampled, the edges of the spectrum have the same scaling with aspect ratio (sample size) as those for the whitened cross-correlation matrix [3]. Thus, in this extremely well sampled limit, the cross-corelation and cross-covariance matrices can both be used to detect a signal. However, the prefactor of this scaling is smaller for the cross-covariance matrix, indicating that whitening using the inverse of the empirically sampled self-covariance matrices introduces additional noise in the spectrum. Further, for sparse data, the cross-correlation cannot be evaluated—even if only one of the two variables is undersampled, where our results suggest that a signal may still be detectable in the cross-covariance. Together, these results suggest that in many cases the cross-covariance may be the most effective tool for detecting the shared signal in a pair of high-dimensional observations.

Appendix A: Calculating the spectrum of the empirical cross-covariance matrix

Here we calculate the spectrum of the $N_X \times N_X$ normalized empirical cross-covariance matrix $\mathbf{C}^T \mathbf{C}$, given by Eq. (4). Given N_X, N_Y, $T \gg 1$, this spectrum can be evaluated using random matrix theory. Parts of this calculation, can be mapped onto previous calculations [6–8] by reinterpreting the meaning of various various. However, for completeness, we present a full, self-contained calculation here.

The nonzero eigenvalues of the NECCM $\mathbf{C}^T \mathbf{C}$ are the same as those of the matrix

$$\mathbf{H} = \frac{1}{\sigma_X^2 \sigma_Y^2 T^2} \left(\mathbf{X} \mathbf{X}^T \right) \left(\mathbf{Y} \mathbf{Y}^T \right)$$

$$= \frac{N_X N_Y}{T^2} W_{X^T} W_{Y^T}$$

$$= \frac{1}{p_X p_Y} W_{X^T} W_{Y^T}. \qquad (A1)$$

Here $\mathbf{W_X}$ and $\mathbf{W_Y}$ are normalized Wishart matrices, given by

$$\mathbf{W_Y} = \frac{1}{T\sigma_Y^2} \mathbf{Y}^T \mathbf{Y}, \qquad (A2)$$

and similar for X. Crucially, $\mathbf{W_X}$ and $\mathbf{W_Y}$ are free matrices (loosely, the appropriate generalization of independence to noncommuting objects, such as matrices).

The spectrum of $\mathbf{H}$, $\rho_{\mathbf{H}}$, can be evaluated from its Stiltjes transform,

$$\mathfrak{h}(z) \equiv \mathfrak{h}_{\mathbf{H}}(z) \equiv \lim_{T \to \infty} \frac{1}{T} \mathrm{Tr}(z\mathbf{I} - \mathbf{H})^{-1}, \qquad (A3)$$

using the formula

$$\rho_{\mathbf{H}}(\lambda) = \frac{1}{\pi} \lim_{\eta \to 0^+} \Im \mathfrak{h}(z = \lambda - i\eta), \qquad (A4)$$

To evaluate this Stiltjes transform, we must introduce the $\mathcal{T}$ and $\mathcal{S}$ transforms, which are useful for evaluating the Stiltjes transform of products of random matrices [2]. Their properties used in further calculations are summarized below.

The $\mathcal{T}$ transform of a matrix A is defined as

$$\mathcal{T}_{\mathbf{A}}(z) = z\mathfrak{g}_{\mathbf{A}}(z) - 1. \qquad (A5)$$

The $\mathcal{T}$ transform, in turn, is used to define the $\mathcal{S}$ transform:

$$\mathcal{S}_{\mathbf{A}}(t) = \frac{t+1}{t\mathcal{T}_{\mathbf{A}}^{-1}(t)}. \qquad (A6)$$

For free matrices $\mathbf{A}$ and $\mathbf{B}$, the $\mathcal{S}$-transform of a product is multiplicative:

$$\mathcal{S}_{\mathbf{AB}}(t) = \mathcal{S}_{\mathbf{A}}(t)\mathcal{S}_{\mathbf{B}}(t). \qquad (A7)$$

Furthermore, for a scalar a,

$$\mathcal{S}_{a\mathbf{A}}(t) = a^{-1}\mathcal{S}_{\mathbf{A}}(t). \qquad (A8)$$

To derive the Stiltjes transform of $\mathbf{H}$, we first evaluate its $\mathcal{S}$ transform. Using Eq. (A7) and Eq. (A8), we write

$$\mathcal{S}_{\mathbf{H}}(t) = \mathcal{S}\left(\frac{1}{p_X p_Y} W_{X^T} W_{Y^T}\right)$$
$$= p_X p_Y \mathcal{S}_{W_{X^T}} \mathcal{S}_{W_{Y^T}}. \qquad (A9)$$

The $\mathcal{S}$-transform of a Wishart matrix is well known [2]:

$$\mathcal{S}_{W_{X^T}} = \frac{1}{1 + p_X t}. \qquad (A10)$$

Now, plugging in the relevant terms for $\mathcal{S}_{W_{X^T}}$ and $\mathcal{S}_{W_{Y^T}}$ in Eq. (A9) using Eq. (A10), we obtain:

$$\mathcal{S}_{\mathbf{H}}(t) = \frac{p_X}{1 + p_X t} \frac{p_Y}{1 + p_Y t}. \qquad (A11)$$

To calculate the spectral density of the matrix of interest we replace the $\mathcal{S}$-transform in Eq. (A11) with the corresponding $\mathcal{T}$-transform by using the relationship in Eq. (A6):

$$\mathcal{T}_{\mathbf{H}}^{-1}(t) = \frac{t + 1(1 + p_X t)(1 + p_Y t)}{t p_X p_Y}. \qquad (A12)$$

We now solve the equation for the functional inverse, $\mathcal{T}^{-1}(\mathcal{T}(z)) = z$, using the definition of the $\mathcal{T}$-transform, Eq. (A5). This gives a cubic equation for the Stieltjes transform:

$$\mathfrak{h}^3 z^2 p_X p_Y + \mathfrak{h}^2 z \left(p_Y(1 - p_X) + p_X(1 - p_Y)\right)$$
$$+ \mathfrak{h}\left((1 - p_X)(1 - p_Y) - z p_X p_Y\right)$$
$$+ p_X p_Y = 0. \qquad (A13)$$

The imaginary part of the roots of the cubic equation give us the density of eigenvalues. The edges of the band $[\lambda_-, \lambda_+]$, for which the density is nonzero, are obtained from the zeros of the discriminant of the cubic equation. For an equation of the form

$$a\mathfrak{h}^3 + b\mathfrak{h}^2 + c\mathfrak{h} + d = 0, \qquad (A14)$$

the discriminant is

$$D = b^2 c^2 - 4ac^3 - 4b^3 d - 27a^2 d^2 + 18abcd, \qquad (A15)$$

where:

$$a = z^2 p_X p_Y, \qquad (A16)$$
$$b = z\left(p_Y(1 - p_X) + p_X(1 - p_Y)\right), \qquad (A17)$$
$$c = \left((1 - p_X)(1 - p_Y) - z p_X p_Y\right), \qquad (A18)$$
$$d = p_X p_Y. \qquad (A19)$$

The density $\rho(\lambda)$ and the edges $\lambda_\pm$ must then be transformed into the density of singular values $\rho(\gamma)$ and the edges $\gamma_\pm$. For this, to get the spectrum of the nonzero part of the SVD of $\mathbf{C}$, we use:

$$\rho_A(z) = 2z\rho_{A^2}(z^2), \qquad (A20)$$

and the edges obey $\gamma_\pm = \sqrt{\lambda_\pm}$.

1. Spectrum of the empirical cross covariance matrix for $T < N_X,\ N_Y$

a. Simplified solutions for $p_X = p_Y$

For $p_X = p_Y$, the cubic equation for the Stieltjes transform, Eq. (A13), reduces to:

$$\mathfrak{h}^3 z^2 p_X{}^2 + \mathfrak{h}^2 z \left(p_X(1 - p_X) + p_X(1 - p_X)\right)$$
$$+ \mathfrak{h}\left((1 - p_X)(1 - p_X) - z p_X{}^2\right) + p_X^2 = 0, \qquad (A21)$$

and the discriminant (Eq. A15) simplifies to

$$D = (4p_X^4 - 12p_X^5 + 12p_X^6 - 4p_X^7)z^3$$

$$+ (-8p_X^6 - 20p_X^7 + p_X^8)z^4 + 4p_X^8 z^5. \qquad \text{(A22)}$$

Solving Eq. (A22) for zeros we find that there are three zeros at $z = 0$ and two zeroes at $\lambda_\pm$. In between these values, the discriminant is negative and thus the solution for $\mathfrak{h}$ has a nonzero imaginary part, giving a nonzero density of eigenvalues. We obtain:

$$\lambda_\pm = \frac{8p_X^2 + 20p_X^3 - p_X^4 \pm p_X^{5/2}(8 + p_X)^{3/2}}{8p_X^4}. \qquad \text{(A23)}$$

For $p_X \to 0$, Eq. (A23) reduces to

$$\lambda_\pm = \frac{1}{p_X^2} \pm \frac{2\sqrt{2}}{p_X^{3/2}}. \qquad \text{(A24)}$$

The singular values of $\mathbf{C}$ have nonzero density between $\gamma_\pm$, where $\gamma_\pm = \sqrt{\lambda_\pm}$. Thus, for small p_X,

$$\gamma_\pm = \sqrt{\frac{1}{p_X^2} \pm \frac{2\sqrt{2}}{p_X^{3/2}}} = \frac{1}{p_X}\sqrt{1 \pm 2\sqrt{2}\sqrt{p_X}}$$
$$\approx \frac{1}{p_X}(1 \pm \sqrt{2p_X}). \qquad \text{(A25)}$$

b. Simplified solutions for $p_X < 1$, $p_Y \ll p_X$

For $p_Y = \epsilon p_X$ under the condition $\epsilon \to 0$, the cubic equation for the Stieltjes transform Eq. (A13) reduces to:

$$\epsilon\mathfrak{h}^3 z^2 p_X^2 + \mathfrak{h}^2 z p_X \left(\epsilon(1 - p_X) + (1 - \epsilon p_X)\right)$$
$$+ \mathfrak{h}\left((1 - p_X)(1 - \epsilon p_X) - z\epsilon p_X^2\right) + \epsilon p_X^2 = 0. \quad \text{(A26)}$$

The discriminant of Eq. (A26) is calculated using Eq. (A15). We then organize this discriminant as a polynomial in z, giving

$$D = 4z^5\epsilon^4 p_X^8 + z^4(\epsilon^2 p_X^6 + \epsilon^3(-10p_X^6 - 10p_X^7)$$
$$+ \epsilon^4(p_X^6 - 10p_X^7 + p_X^8)) + z^3(\epsilon(-2p_X^4 - 2p_X^5)$$
$$+ \epsilon^2(8p_X^4 - 4p_X^5 + 8p_X^6) + \epsilon^3(-2p_X^4 - 4p_X^5 - 4p_X^6 - 2p_X^7)$$
$$+ \epsilon^4(-2p_X^5 + 8p_X^6 - 2p_X^7)) + z^2(p_X^2 - 2p_X^3 + p_X^4$$
$$+ \epsilon(-2p_X^2 + 2p_X^3 + 2p_X^4 - 2p_X^5)$$
$$+ \epsilon^2(p_X^2 + 2p_X^3 - 6p_X^4 + 2p_X^5 + p_X^6)$$
$$+ \epsilon^3(-2p_X^3 + 2p_X^4 + 2p_X^5 - 2p_X^6) + \epsilon^4(p_X^4 - 2p_X^5 + p_X^6)). \quad \text{(A27)}$$

Each term is of the form $f_n(\epsilon)z^n$. As $\epsilon \to 0$, we may expand each $f_n(\epsilon)$ to the lowest nontrivial order in ϵ. Collecting the lowest-order terms for each power of z, the discriminant in Eq. (A27) reduces to:

$$D \approx z^2 \left[p_X^2(1 - p_X)^2 - 2(p_X^4 + p_X^5)\epsilon z + p_X^6\epsilon^2 z^2 \right.$$
$$\left. + 4p_X^8\epsilon^4 z^3\right]. \quad \text{(A28)}$$

We seek positive roots $z_\pm(\epsilon)$ of the right-hand group of terms (the equation has a single negative root, but since the eigenvalues of $\mathbf{H}$ are positive by construction, this corresponds to a spurious root of the equation for $\mathfrak{h}$). This requires cancellation of at least two terms. That is, at least two terms of opposite signs must be of the same order in ϵ. We see that this can only happen if $z \sim \epsilon^{-1}$ or $z \sim \epsilon^{-3/2}$. In both of these possible cases, the final term is subleading and can be neglected. Thus, in this limit, we seek the roots of

$$D \approx (p_X^2 - 2p_X^3 + p_X^4)z^2 - 2(p_X^4 + p_X^5)z^3\epsilon + z^4 p_X^6 \epsilon^2. \quad \text{(A29)}$$

We solve Eq. (A29) for zeros. The 4th-order equation has four zeroes. Two of the zeros are $z = 0$, and the other two, $\lambda_\pm$, are

$$\lambda_\pm = \frac{1 + p_X \pm 2\sqrt{p_X}}{\epsilon p_X^2}$$
$$\approx \frac{1 + p_X \pm 2\sqrt{p_X}}{p_X p_Y}. \qquad \text{(A30)}$$

Thus the density of eigenvalues for for SVD of $\mathbf{C}$ will be nonzero between $\gamma_\pm = \sqrt{\lambda_\pm}$, such that

$$\gamma_\pm \approx \sqrt{\frac{1 + p_X \pm 2\sqrt{p_X}}{p_X p_Y}}. \qquad \text{(A31)}$$

c. Simplified solutions for $p_X, p_Y \ll 1$

For $p_Y = \alpha p_X$ under the condition $p_X \to 0$ and $\alpha < 1$, the cubic equation for the Stieltjes transform Eq. (A13) reduces to:

$$\alpha\mathfrak{h}^3 z^2 p_X^2 + \mathfrak{h}^2 z p_X (\alpha + 1) + \mathfrak{h}\left(1 - z\alpha p_X^2\right) + \alpha p_X^2 = 0. \quad \text{(A32)}$$

The discriminant of Eq. (A32) is calculated using Eq. (A15). Written as a polynomial in z, it is

$$D = 4z^5\alpha^4 p_X^8 + z^4(\alpha^2 p_X^6 - 10\alpha^3 p_X^6 + \alpha^4 p_X^6 - 18\alpha^3 p_X^7$$
$$- 18\alpha^4 p_X^7 - 27\alpha^4 p_X^8) + z^3(-2\alpha p_X^4 + 8\alpha^2 p_X^4 - 2\alpha^3 p_X^4$$
$$- 4\alpha p_X^5 + 6\alpha^2 p_X^5 + 6\alpha^3 p_X^5 - 4\alpha^4 p_X^5)$$
$$+ z^2(p_X^2 - 2\alpha p_X^2 + \alpha^2 p_X^2). \quad \text{(A33)}$$

As $p_X \to 0$, the contribution of higher-order terms for each power of z to the final solution will be negligible. Collecting the lowest order terms in p_X for each power of z, the discriminant in Eq. (A33) reduces to

$$D = 4z^5\alpha^4 p_X^8 + z^4(\alpha^2 p_X^6 - 10\alpha^3 p_X^6 + \alpha^4 p_X^6)$$
$$+ z^3(-2\alpha p_X^4 + 8\alpha^2 p_X^4 - 2\alpha^3 p_X^4) +$$
$$z^2(p_X^2 - 2\alpha p_X^2 + \alpha^2 p_X^2). \quad \text{(A34)}$$

We solve Eq. (A34) for zeros. The 5th-order equation has 5 zeroes (counting their multiplicities). Two of the zeroes are at $z = 0$, one is at $z = \frac{-(1-\alpha)^2}{4\alpha^2 p_X^2} < 0$. Thus, the other two are $\lambda_\pm$. Taking the condition $D < 0$, we find that nonzero density requires $\lambda \in [\lambda_-, \lambda_+]$. In particular, we find the solution

$$\lambda_\pm = \frac{1 \pm 2\sqrt{p_X(1+\alpha)}}{\alpha p_X^2}. \tag{A35}$$

The nonzero density of eigenvalues for SVD of $\mathbf{C}$ will be between $\gamma_\pm = \sqrt{\lambda_\pm}$:

$$\begin{aligned}
\gamma_\pm = \sqrt{\lambda_\pm} &= \sqrt{\frac{1 \pm 2\sqrt{p_X(1+\alpha)}}{\alpha p_X^2}} \\
&= \sqrt{\frac{1 \pm 2\sqrt{p_X + p_Y}}{p_Y p_X}} \\
&\approx \frac{1 \pm \sqrt{p_Y + p_X}}{\sqrt{p_Y p_X}}. \tag{A36}
\end{aligned}$$

2. Spectrum of the empirical cross covariance matrix when $T > N_X, N_Y$

a. Simplified solutions for $p_X = p_Y$

For $p_X = p_Y$, the discriminant takes the same form as in the case $T < N_X, N_Y$ (Eq. A22). That is,

$$D = (4p_X^4 - 12p_X^5 + 12p_X^6 - 4p_X^7)z^3$$
$$+ (-8p_X^6 + 20p_X^7 + p_X^8)z^4 + 4p_X^8 z^5. \tag{A37}$$

In this case, however, the identities of the roots that determine $\lambda_\pm$ are different from the case $T < N_X, N_Y$. Specifically, Eq. (A37) has three zeros at $z = 0$ and one zero each at $z_- = \frac{8p_X^2 + 20p_X^3 - p_X^4 - p_X^{5/2}(8+p_X)^{3/2}}{8p_X^4}$ and $z_+ = \frac{8p_X^2 + 20p_X^3 - p_X^4 + p_X^{5/2}(8+p_X)^{3/2}}{8p_X^4}$. The root $z_- < 0$, and the squares of the singular values are always non-negative. Thus the lower edge is $\lambda_- = 0$, and $\lambda_+ = z_+ = \frac{8p_X^2 + 20p_X^3 - p_X^4 + p_X^{5/2}(8+p_X)^{3/2}}{8p_X^4}$. Thus the upper edge of the SVD spectrum is $\gamma_+ = \sqrt{\lambda_+}$. For $p_X \gg 1$,

$$\lambda_+ \approx -\frac{1}{8} + \left(\frac{(8+p_X)^{3/2}}{8p_X^{3/2}}\right) \tag{A38}$$

$$\approx \frac{3}{2p_X}. \tag{A39}$$

Thus,

$$\gamma_+ = \sqrt{\frac{3}{2p_X}}. \tag{A40}$$

[1] V. Marchenko and L. Pastur, Mat. Sb **72**, 507 (1967), in Russian.
[2] M. Potters and J.-P. Bouchaud, *A First Course in Random Matrix Theory: For Physicists, Engineers and Data Scientists* (Cambridge University Press, 2020).
[3] J.-P. Bouchaud, L. Laloux, M. A. Miceli, and M. Potters, The European Physical Journal B **55**, 201 (2007).
[4] F. Benaych-Georges, J.-P. Bouchaud, and M. Potters, The Annals of Applied Probability **33**, 1295 (2023).
[5] N. Firoozye, V. Tan, and S. Zohren, Journal of Banking & Finance **154**, 106952 (2023).
[6] P. Fleig and I. Nemenman, Phys. Rev. E **106**, 014102 (2022).
[7] J. W. Rocks and P. Mehta, Phys. Rev. E **106**, 025304 (2022).
[8] Z. Burda, A. Jarosz, G. Livan, M. A. Nowak, and A. Swiech, Phys. Rev. E **82**, 061114 (2010).
[9] E. Abdelaleem, A. Roman, K. M. Martini, and I. Nemenman, Transactions on Machine Learning Research (2024).